Electronic Supplementary Material (ESI) for Environmental Science: Processes & Impacts.

Supplementary information

Adsorption of progesterone onto microplastics and its desorption in simulated gastric and intestinal fluids

Cécilia Siri[a], Yang Liu [a,b], Thibault Masset [a], William Dudefoi [c,d], Dean Oldham [d], Matteo Minghetti [d], Dominique Grandjean[a] and Florian Breider* [a]

Methods

Analytical method

Progesterone quantification was performed with an LC-MS/MS Acquity Ultra Performance from Waters equipped with a HSS T3 Acquity C18 reversed phase column from Waters (2.1mm IS, 100mm length). The LC was connected to a TQ MS Xevo employing ESI as ionization source (ES+). The masses of progesterone (315.23 Da) and progesterone-$^{13}C_3$ (318.28 Da) daughter ions are 96.97 and 108.94 Da and 99.90 and 111.90 Da, respectively. The collision gas was argon. The eluent was a mix 95% H_20 MQ - 5% ACN : 95% ACN - 5% H_20 MQ with a composition 30:70. The flow rate was set at 0.5ml/min and the total run time was 10min. The LOD and the LOQ of the experimental method have been determined to be 1.25 ng/ml and 4.2 ng/ml, respectively.

Characterization of microplastics and fluids

The FTIR spectra of each plastic type were obtained using a FTIR spectrometer equipped with a diamond ATR crystal (Perkin-Emler Spectrum Two). The measurements were realized from 900 to 4000 cm^{-1} with a resolution of 2 cm^{-1}. The morphology of pristine microplastics was characterized using a scanning electron microscope (Zeiss Gemini SEM 300). Microplastics were 10 nm-gold coated with a Quorum apparatus. One particle for each plastic type has been imaged with 34-fold magnification. The all zoom-in images were taken with different magnifications. The energy of electrons was 5.00 keV and the aperture size was 30.00 µm. The water contact angles (WCA) were measured using the sessile drop method on a EasyDrop device (Kruss GmBH) under ambient condition. The volume of the drop was set to around 9µL. The contact angle of the three different fluids was measured using LDPE as a substrate with the same parameters. For the contact angle measurements of the different microplastics, an accessory adapted to powders was used. Differential scanning calorimetry (DSC) measurements were performed on a DSC 8000 device (Perkin-Emler) with a heating rate of 10°C/min in heating mode and 5°C in a cooling mode. The maximum temperature was set at 240°C for all plastic types, except for PS for which the temperature was set to 360°C. Each sample was measured twice. The Zeta potential of the biological fluids was measured by dynamic light scattering using a (Zetasizer Malvern), from which the size of particles in the fluids were determined. Three measurements of fifteen runs each have been performed for each fluid type.

Extraction from microplastics

20mg of each plastic type were balanced in 10mL vials and 5mL of MeOH was added and shaked for 30min. Three replicates were performed for each plastic type. Then the vials were filtered on solid phase extraction (SPE) columns and 3mL of MeOH was added to microplastics to further rinse them. The process was repeated with hexane. The organic phases collected were concentrated under N_2 flux at 40 ◦C until it remains 0.5 mL of liquid. The latter was transferred in 1.5mL vial and the vial was further rinsed with 1mL MeOH which was transferred in the 1.5 mL vial. Those vials were further concentrated under N_2 flux until dryness. 0.25 mL of MeOH was added with 0.15 mL eluent and 0.1 mL of internal standard before LC-MS/MS analysis**.**

Theory

Concerning the adsorption, the equations of the pseudo-first order model and the pseudo-second order model are presented below, respectively.

$$\ln(q_{eq} - q_t) = \ln(q_{eq}) - kt$$

Where q_{eq} and q_t are defined as the adsorption capacity in mg/g at equilibrium and at a time *t*, respectively. *k* is the rate constant in h^{-1}.

$$t/q_t = 1/kq_{eq}^2 + 1/q_{eq}\, t$$

The intra-particulate diffusion model (IDM) is suitable to describe liquid/solid kinetics where diffusion is the rate-limiting step. **(1)**

$$q_t = kt^{1/2} + x_i$$

Where q_t represents the adsorption capacity at a time *t* and x_i a constant.
The isotherms fitting models are Langmuir and Freundlich models, usually employed to describe adsorption isotherms. (2) (3) (4)

$$1/q_{eq} = 1/K_L * Q_m * C_{eq} + 1/Q_m$$

Where q_{eq} (mg/g) and C_{eq} (mg/L) correspond to the adsorption capacity at equilibrium and the pollutant concentration at equilibrium respectively. Q_m is the maximal adsorption capacity of the adsorbent (mg/g) and K_L is the Langmuir adsorption constant (L/mg).

$$\log q_{eq} = logK_F + 1/n * logC_{eq}$$

n is the Freundlich coefficient and provides an indication about the linearity of the isotherm. It also indicates the relative distribution of the energy and the heterogeneity of the adsorbate sites. (5) If $1< n < 10$, the adsorption is said favorable and if $n < 1$, the adsorption is said co-operative. K_F is the Freundlich constant and q_{eq} (mg/g) and C_{eq} (mg/L) have the same definition as above.

Characterization of microplastics by ATR-FTIR

On the HDPE spectrum (see figure 0a), the band around 2929 cm^{-1} corresponds to the CH2 asymmetric stretching, while the peak around 2850 cm^{-1} is due to CH_2 symmetric stretching. Thus, the peak around 1470 cm^{-1} was assigned to the bending deformation. **(6)** For PP (see figure 0b), the two peaks around 1460 cm^{-1} were assigned to the bending of the methylene group. At higher wavenumber, the asymmetric and symmetric stretching of the methylene group can be assigned to the smallest wavenumbers, while the asymmetric and symmetric stretching of CH_3 peaks were higher in wavenumbers. Finally, for PS, (see figure 0c) one found the same peaks around 1470 cm^{-1} corresponding to the bending of the methylene group. The peak at around 1600 cm^{-1} corresponds to the aromatic ring stretching of the phenyl group. In higher wavenumbers, the two first peaks were similar as the previously observed ones, corresponding to the asymmetric and symmetric stretching of the methylene. However, the last two peaks at the highest wavenumbers are typical of aromatic ring stretching.

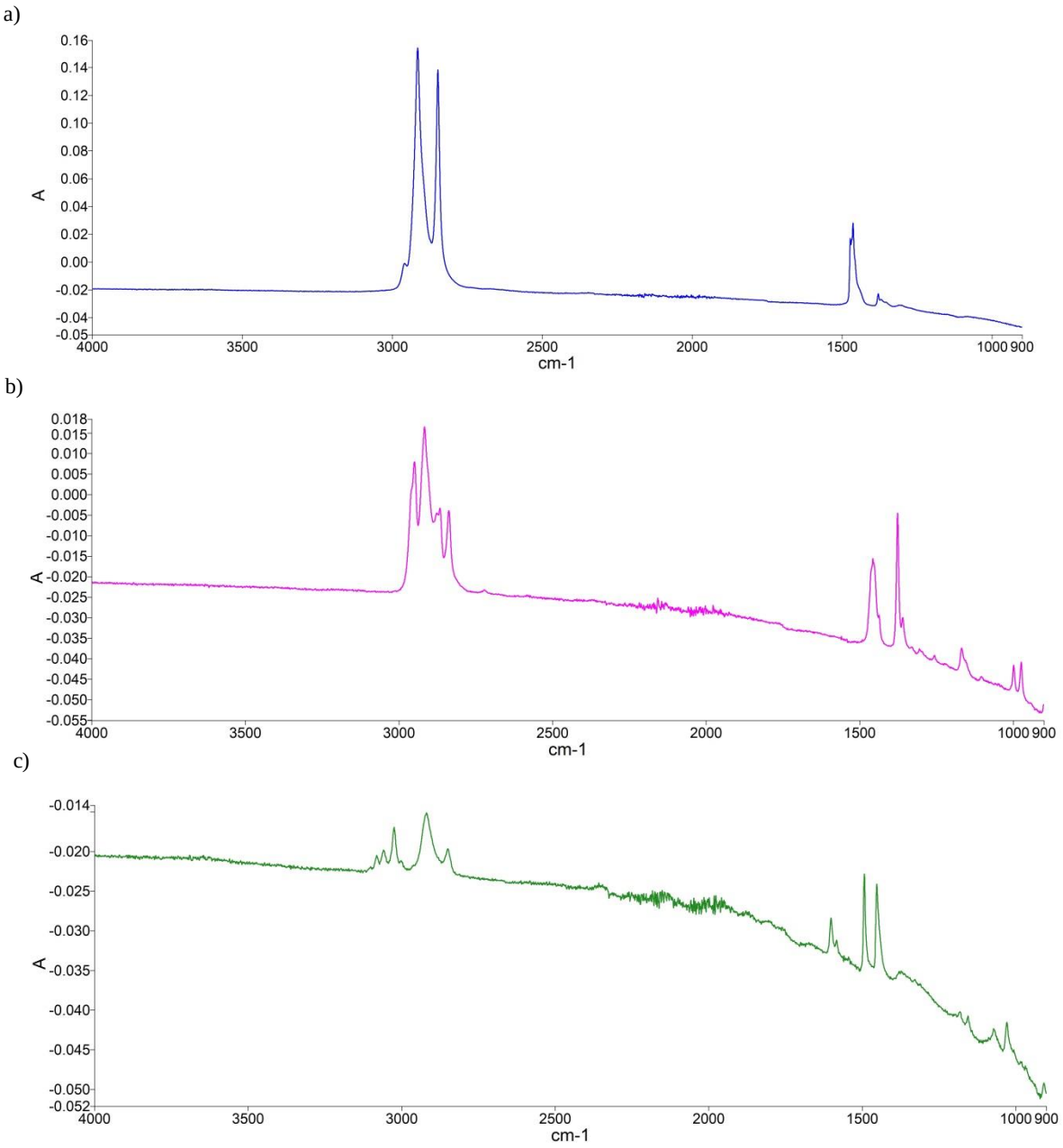

Figure S1. FTIR spectra of (a)HDPE, (b) PP and (c) PS microplastics.

Figures and Tables

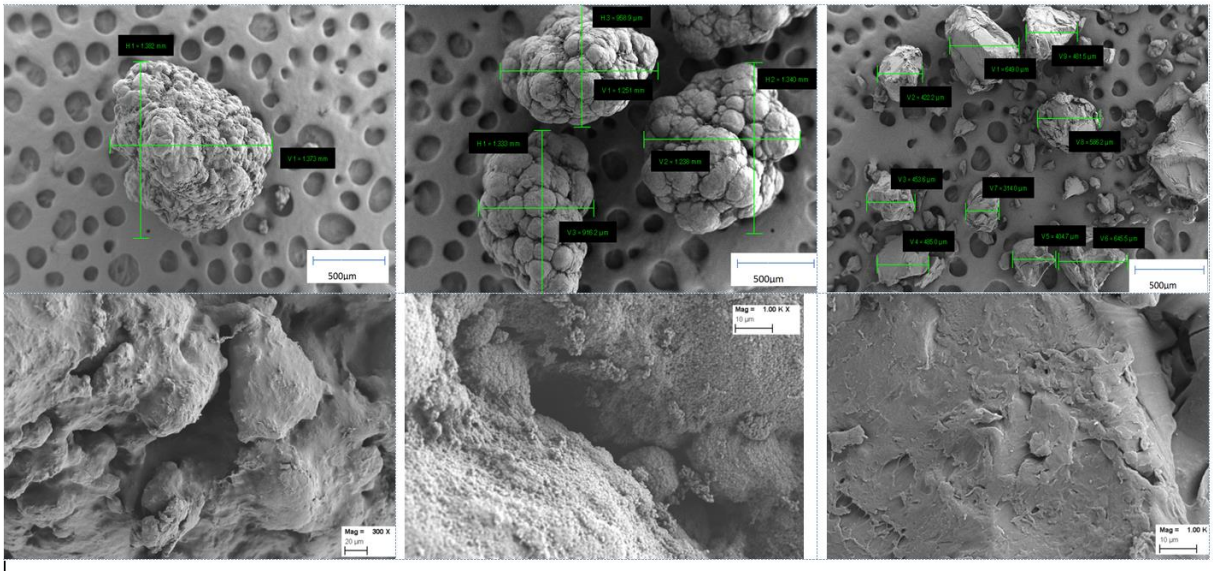

Figure S2. SEM images of PE, PP and PS microplastics at 34X magnification and higher magnifications for the zoom-in images. The corresponding magnifications are indicated in the white box.

Plastic type	HDPE	LDPE	PP	PS
Experimental WCA (°)	-	120.6±0.3	125.5±4.6	117.6±1.4
Literature WCA (°) (7)	108.8±3.8	95.6±3.2	106.3±2.3	95.7±1.4
Literature WCA (°) (8)	-	-	-	125.6
Literature WCA (°) (9)	-	137	-	-
Literature WCA (°) (10)	-	91	95	-
Melting points (°C)	118	-	150	-
Crystallinity (%)	15.9	-	39.5	-

Table S1. Water contact angles and thermodynamics characteristics of three plastic types. Comparison between WCA found experimentally and the ones form literature.

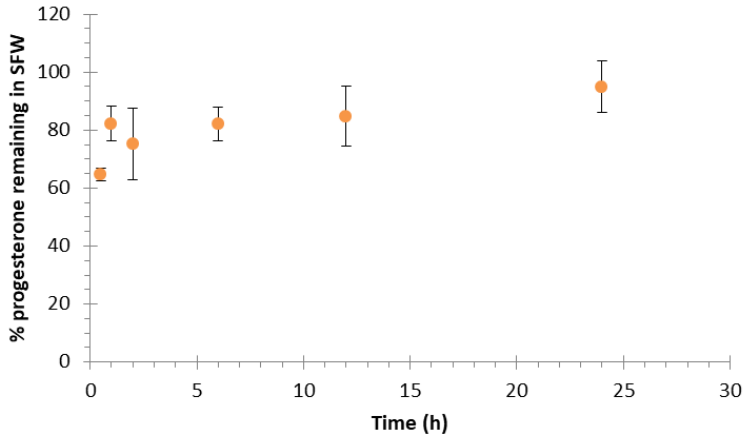

Figure S3. Progesterone stability in SFW. Experiments are done in triplicate.

In order to evaluate the stability of the progesterone in SFW, we compared the incertitude of the percentage of progesterone remaining in the SFW for each time point with the standard deviation of the six average values of progesterone remaining in SFW. Since the latter is smaller than the first one, we concluded that the progesterone is stable in SFW.

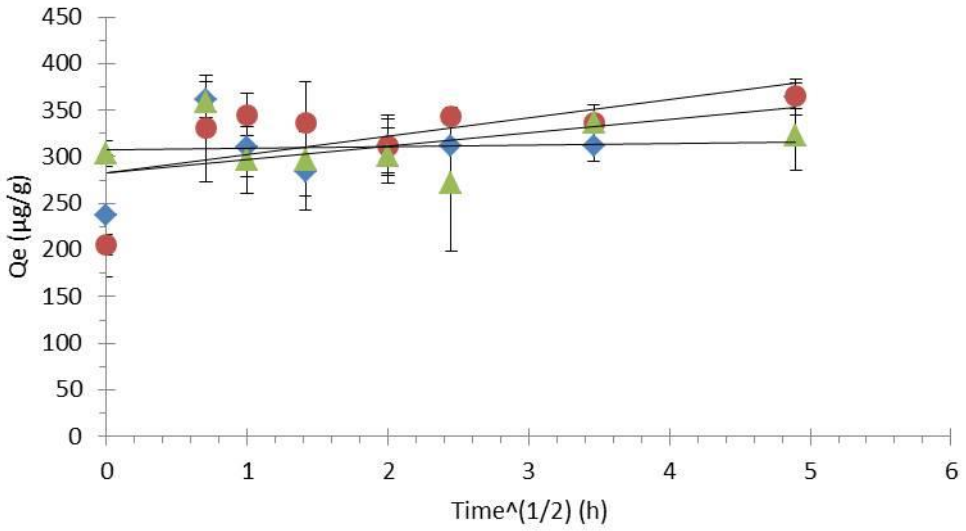

Figure S4. Intraparticulate diffusion model fitting of progesterosorption kinetics on the different types of microplastics. PE is represented by red squares with R^2=0.3945, PP by green triangles with R^2=0.0112 and PS by blue diamonds with R^2=0.3086.

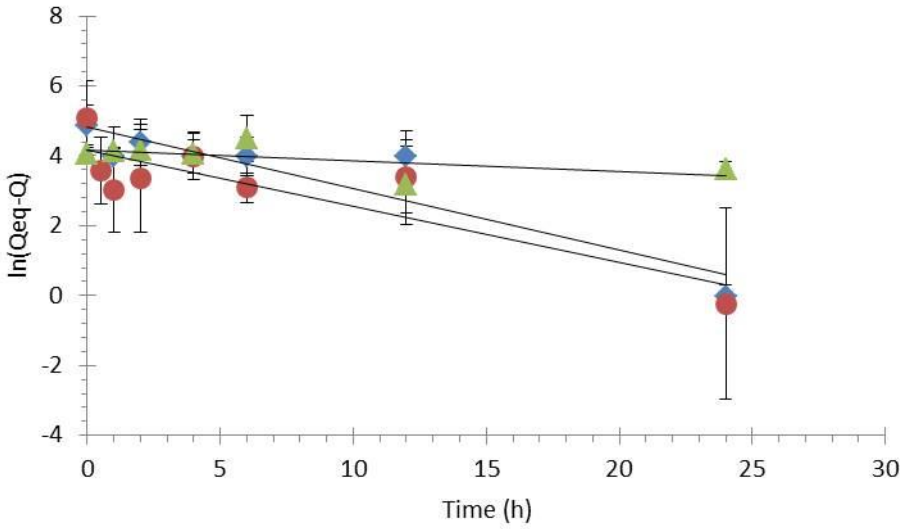

Figure S5. Pseudo-first order model fitting of progesterone sorption kinetics on the different types of microplastics. PE is represented by red squares with R^2=0.7438, PP by green triangles with R^2=0.3762 and PS by blue diamonds with R^2=0.8416.

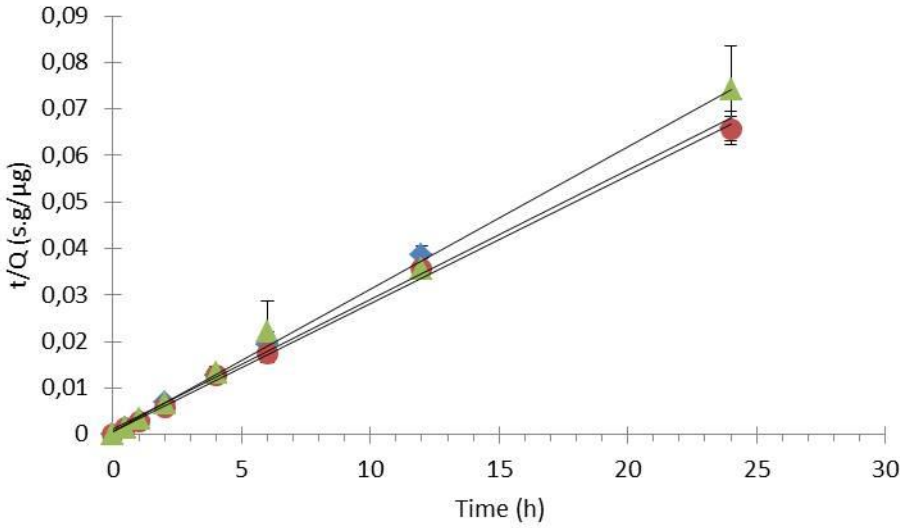

Figure S6. Pseudo-second order model fitting of progesterone sorption kinetics on the different types of microplastics. PE is represented by red squares with R^2=0.9979, PP by green triangles with R^2=0.9969 and PS by blue diamonds with R^2=0.993.

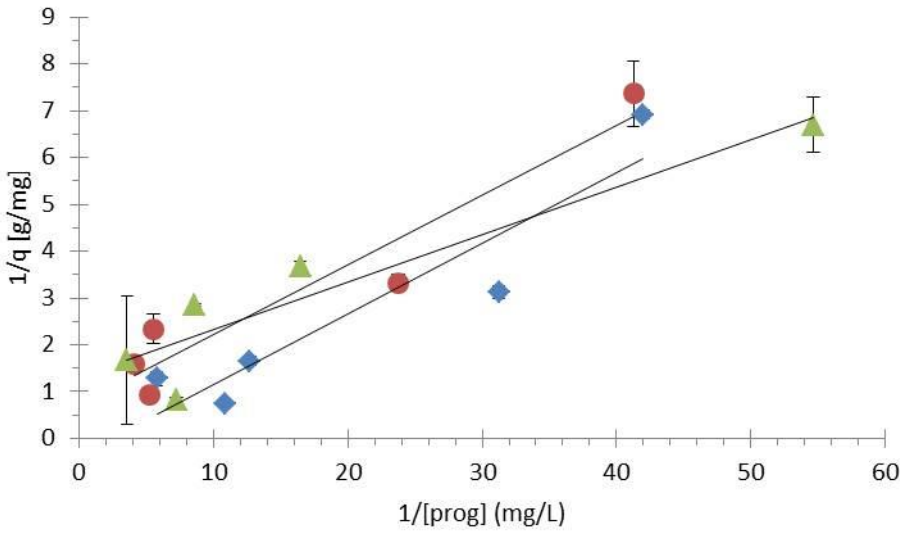

Figure S7. Sorption isotherm of progesterone on the three plastic types fitted with Langmuir isotherm. PE is represented by the red squares, PP by green triangles and PS by the blue diamonds.

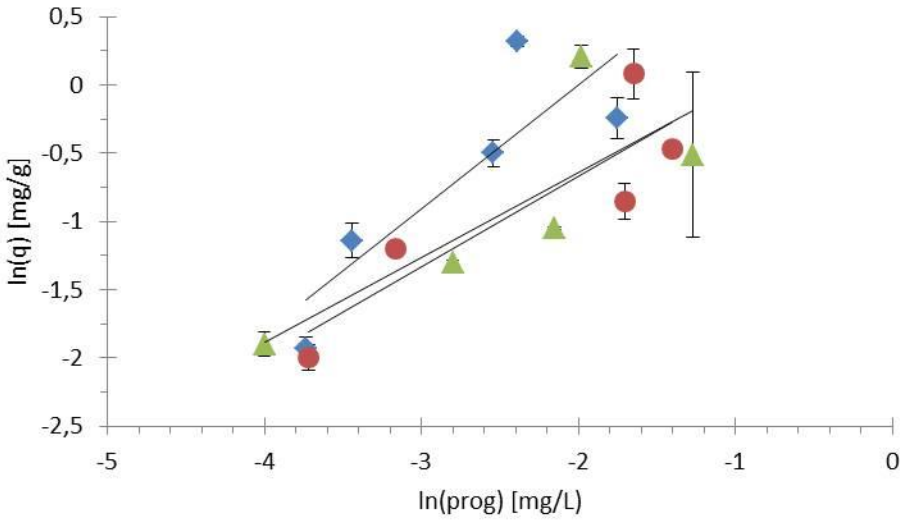

Figure S8. Sorption isotherm of progesterone on the three plastic types fitted with Freundlich isotherm. PE is represented by the red squares, PP by green triangles and PS by the blue diamonds.

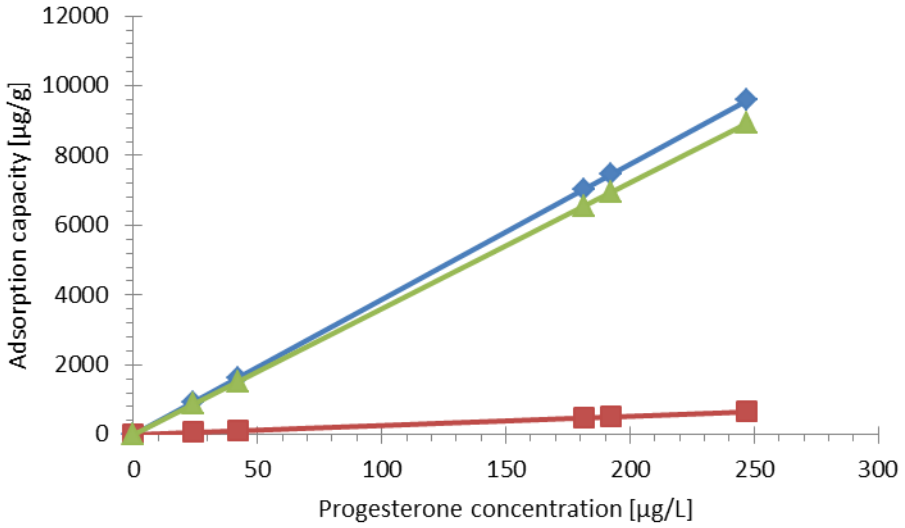

Figure S9. Contribution of partitioning and adsorption respectively to the total sorbed amount of progesterone on PE. The blue diamonds correspond to the total amount sorption capacity, the red squares the partitioning contribution and the green triangles to the adsorption contribution

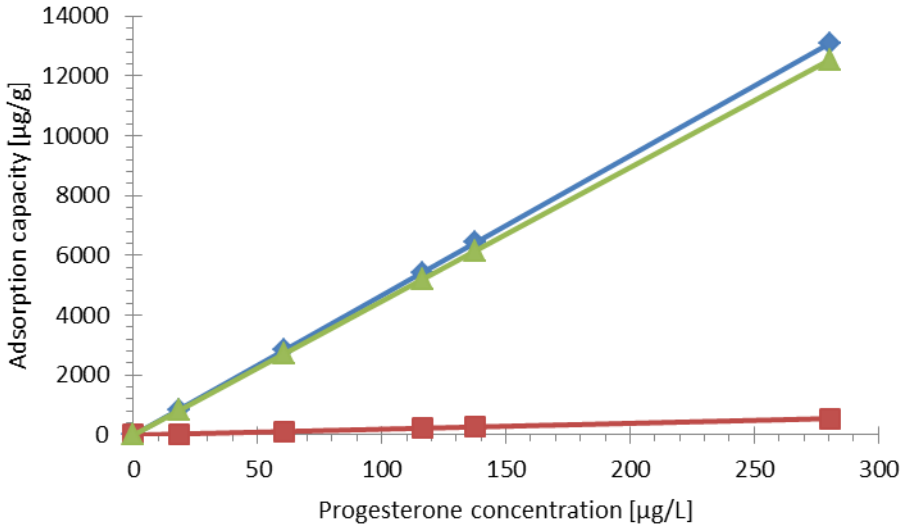

Figure S10. Contribution of partitioning and adsorption respectively to the total sorbed amount of progesterone on PP. The blue diamonds correspond to the total amount sorption capacity, the red squares the partitioning contribution and the green triangles to the adsorption contribution

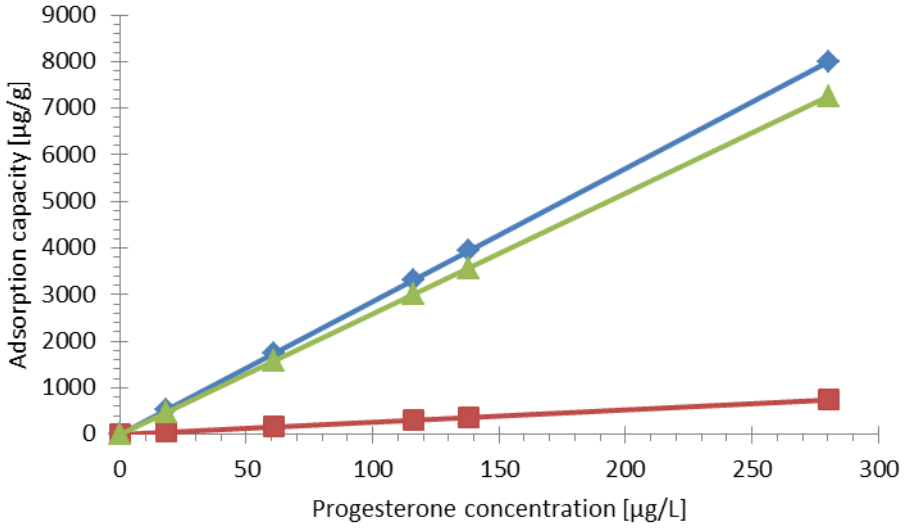

Figure S11. Contribution of partitioning and adsorption respectively to the total sorbed amount of progesterone on PS. The blue diamonds correspond to the total amount sorption capacity, the red squares the partitioning contribution and the green triangles to the adsorption contribution

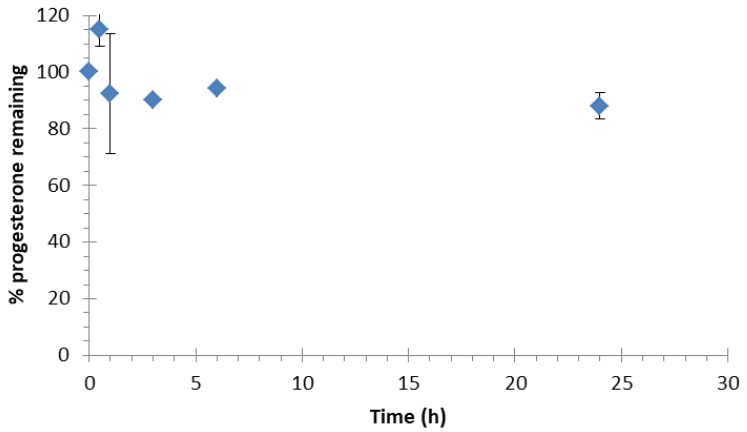

Figure S12. Progesterone stability in SGF. Experiments are done in triplicate.

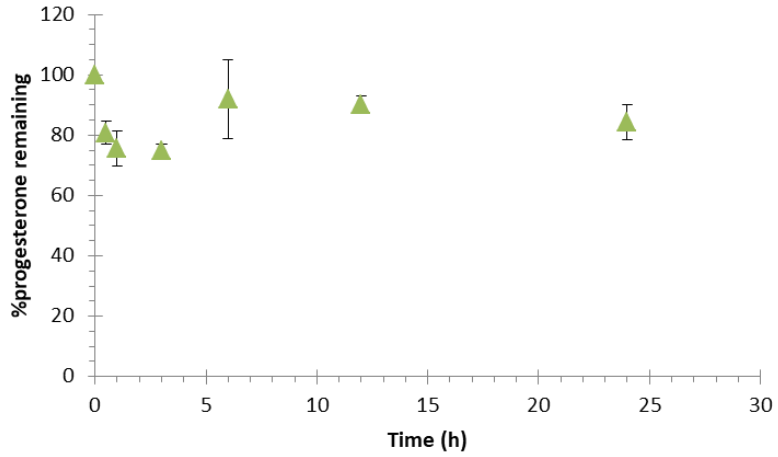

Figure S13. Progesterone stability in SIF. Experiments are done in triplicate.

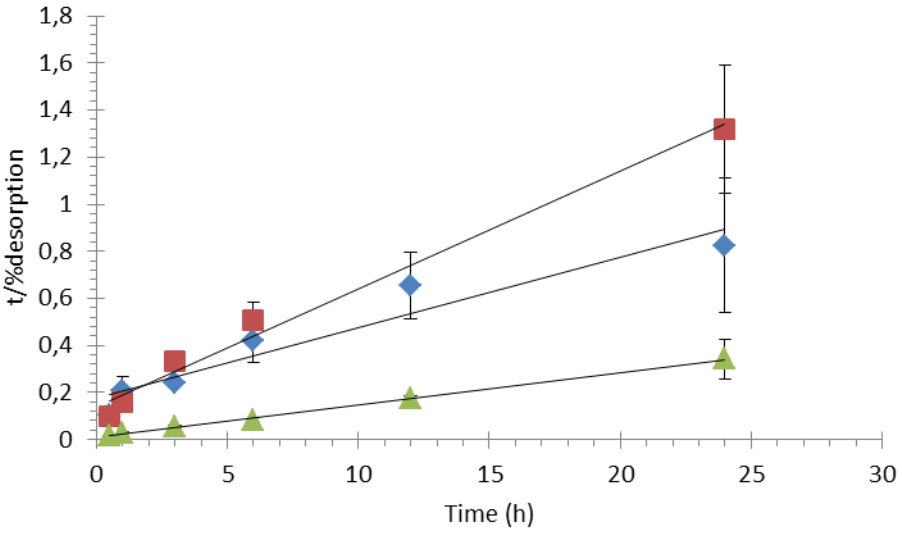

Figure S14. Desorption kinetics of progesterone from PE fitted with the linearized form of the pseudo second order model. The SFW is represented by blue diamonds with R^2 = 0.9221, SGF by red squares with R^2 = 0.9876 and SIF by green triangles with R^2 = 0.9984.

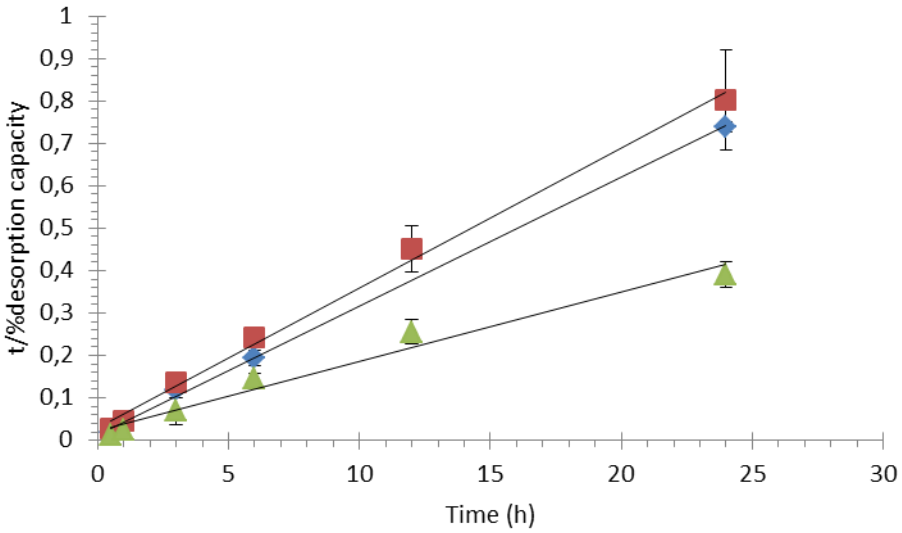

Figure S15. Desorption kinetics of progesterone from PP fitted with the linearized form of the pseudo second order model. The SFW is represented by blue diamonds with R^2 = 0.9989, SGF by red squares with R^2 = 0.9956 and SIF by green triangles with R^2 = 0.9714.

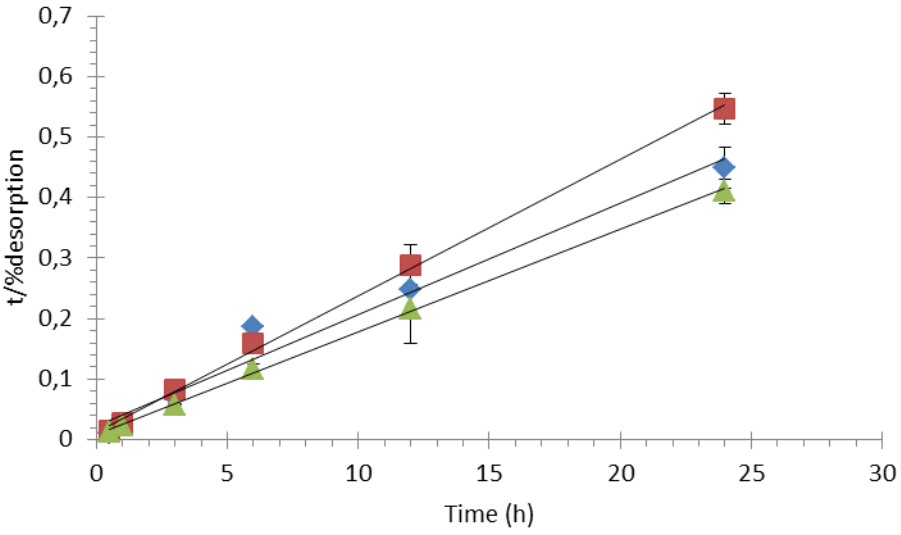

Figure S16. Desorption kinetics of progesterone from PS fitted with the linearized form of the pseudo second order model. The SFW is represented by blue diamonds with R^2 = 0.9724, SGF by red squares with R^2 = 0.9981 and SIF by green triangles with R^2 = 0.9989.

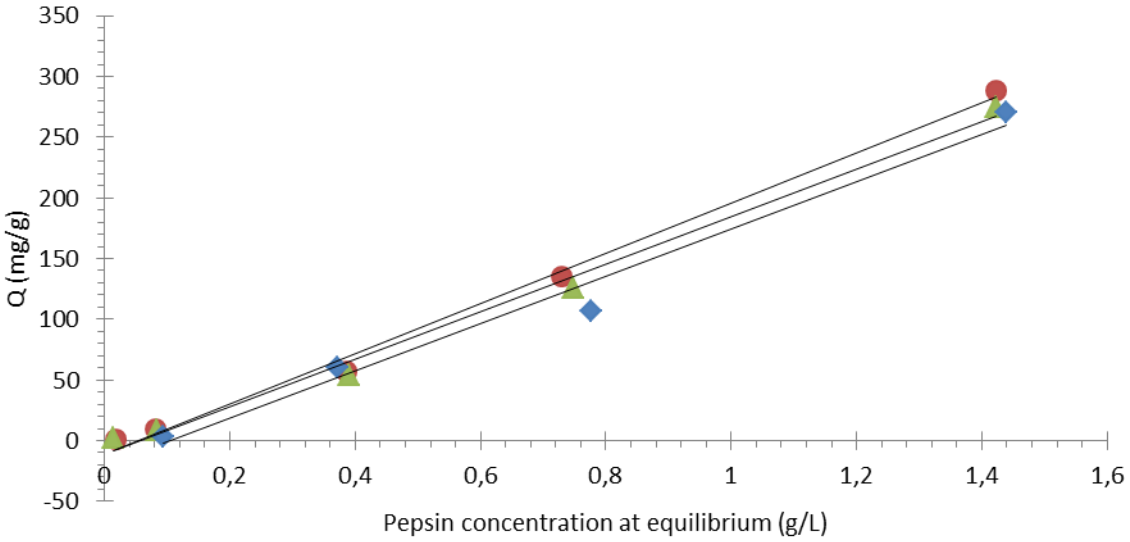

Figure S17. Pepsin sorption capacity onto virgin microplastics. PE are represented by red squares with R^2 = 0.9954. PP are represented by green triangles with R^2=0.9922 and finally PS are represented by blue diamonds with R^2 = 0.9804

To investigate if the pepsin sorption on microplastics is non-negligible, a one way ANOVA test has been performed using a confidence level of 0.95 and Origin as software. The results of this statistical test showed that the sorption is significant.

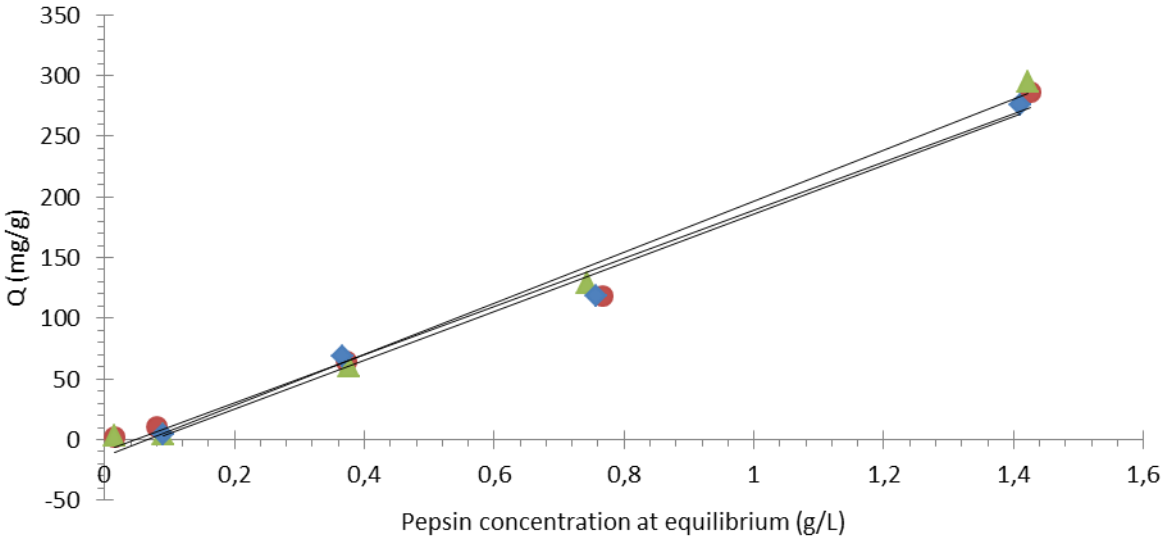

Figure S18. Pepsin sorption capacity onto progesterone-adsorbed microplastics. PE are represented by red squares with R^2 = 0.9839. PP are represented by green triangles with R^2=0.9915 and finally PS are represented by blue diamonds with R^2 = 0.9873

Parameters	Q_{eq} (µg/g)	F_{des} (12h)	C_{prog} (mg/L)	C_{MP} (mg/L)	W (kg)
Values	350	0.73 (PE)	0.4	0.25	1

Table S2. Values of the parameters used for the daily intake model

An organism of 1kg can model the rainbow trout, well reported in literature as a model fish. The progesterone concentration chosen is the same than the one used in the sorption experiments in this study. The parameters Qeq and Fdes correspond to the values found in this study. The microplastics concentration is the one reported in literature to correspond to the microplastics concentration in the environment. (11)

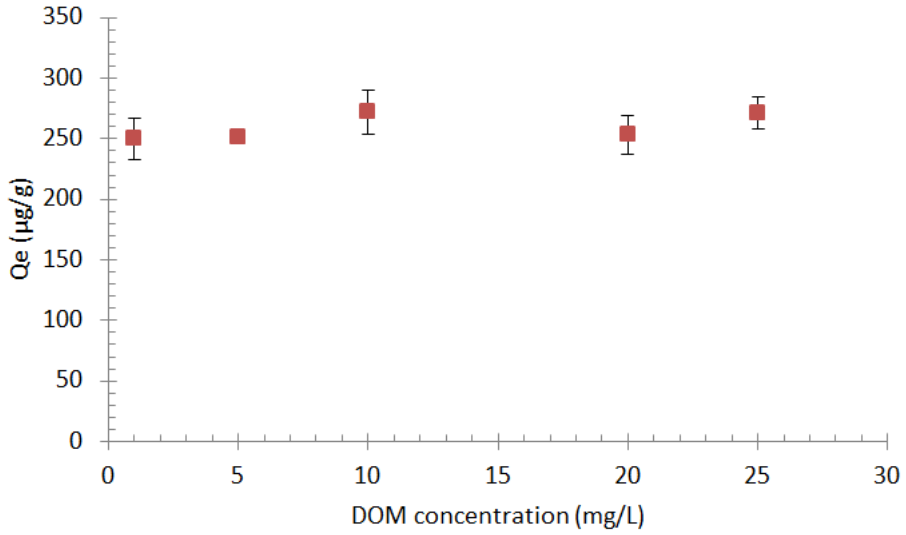

Figure S19. Sorption of progesterone on PE in presence of DOM

Microplastic types	PE	PP	PS	Without MP
Recovery rate (%)	68.8	64.9	79.64	100.6

Table S3. Recovery rates of the progesterone after extraction procedure

References

1. Simonin JP, Bouté J, Simonin JP, Bouté J. Intraparticle diffusion-adsorption model to describe liquid/solid adsorption kinetics. Rev Mex Ing Quím. 2016;15(1):161–73.

2. Guo X, Wang J. The chemical behaviors of microplastics in marine environment: A review. Mar Pollut Bull. 2019 May 1;142:1–14.

3. Lu J, Wu J, Wu J, Zhang C, Luo Y. Adsorption and Desorption of Steroid Hormones by Microplastics in Seawater. Bull Environ Contam Toxicol [Internet]. 2020 Jan 7 [cited 2020 Apr 9]; Available from: http://link.springer.com/10.1007/s00128-020-02784-2

4. Liu G, Zhu Z, Yang Y, Sun Y, Yu F, Ma J. Sorption behavior and mechanism of hydrophilic organic chemicals to virgin and aged microplastics in freshwater and seawater. Environ Pollut. 2019 Mar;246:26–33.

5. Ayawei N, Ebelegi AN, Wankasi D. Modelling and Interpretation of Adsorption Isotherms [Internet]. Vol. 2017, Journal of Chemistry. Hindawi; 2017 [cited 2020 Aug 25]. p. e3039817. Available from: https://www.hindawi.com/journals/jchem/2017/3039817/

6. Gulmine JV, Janissek PR, Heise HM, Akcelrud L. Polyethylene characterization by FTIR. Polym Test. 2002 Jan 1;21(5):557–63.

7. Liu X, Xu J, Zhao Y, Shi H, Huang C-H. Hydrophobic sorption behaviors of 17β-Estradiol on environmental microplastics. Chemosphere. 2019 Jul;226:726–35.

8. Ding L, Mao R, Ma S, Guo X, Zhu L. High temperature depended on the ageing mechanism of microplastics under different environmental conditions and its effect on the distribution of organic pollutants. Water Res. 2020 May 1;174:115634.

9. Shen X-C, Li D-C, Sima X-F, Cheng H-Y, Jiang H. The effects of environmental conditions on the enrichment of antibiotics on microplastics in simulated natural water column. Environ Res. 2018 Oct 1;166:377–83.

10. Chen Q, Wang Q, Zhang C, Zhang J, Dong Z, Xu Q. Aging simulation of thin-film plastics in different environments to examine the formation of microplastic. Water Res. 2021 Sep 1;202:117462.

11. Liu P, Wu X, Liu H, Wang H, Lu K, Gao S. Desorption of pharmaceuticals from pristine and aged polystyrene microplastics under simulated gastrointestinal conditions. J Hazard Mater. 2020 Jun 15;392:122346.